DISCRETE AND CONTINUOUS DYNAMICAL SYSTEMS
Supplement Volume 2007

Website: www.aimSciences.org

pp. 1–10

NONLINEAR DYNAMICS ON CENTRE MANIFOLDS DESCRIBING TURBULENT FLOODS: k-ω MODEL

D. J. Georgiev, A. J. Roberts and D. V. Strunin

Department of Mathematics and Computing
University of Southern Queensland
Toowoomba, Queensland 4350, Australia

Abstract. In shallow turbulent flows such as floods and tsunami vertical mixing tends to smooth out the flow characteristics in cross-sectional direction. The evolution of the average cross-flow characteristics presents considerable interest. We model such flows using the k-ω model of turbulence in the framework of the centre manifold theory. We tested the approach on an artificial diffusion problem for which an exact analytical solution is derived. Then we apply the method to model the turbulent flows and deduced the evolution equations for the average velocity, turbulent energy and its rate of dissipation.

1. **Introduction: the k-ω model.** The k-ω model of turbulence of Wilcox [7] performs well near boundaries [3] and is therefore useful for the shallow flows. It is written in terms of three ensemble averaged quantities: the average turbulent kinetic energy k, the rate of energy dissipation ω and the velocity u. For brevity we use the notation $\boldsymbol{T} \equiv (u, k, \omega) = \begin{bmatrix} u & k & \omega \end{bmatrix}^T$. The coefficient of turbulent diffusion

$$\nu \equiv \frac{k}{\omega} \,. \tag{1}$$

In this work we neglect downstream variations, so that we only explore the time evolution of the vertical structure of the turbulent flow:

$$\boldsymbol{T} = \boldsymbol{T}(y, t) \,, \quad y \in [0, \eta] \,, \quad t \in [0, \infty] \,, \tag{2}$$

where η is the height of the free surface above the ground.

The k-ω model has the form

$$\frac{\partial u}{\partial t} = \frac{\partial}{\partial y}\left(\nu \frac{\partial u}{\partial y}\right) + g_x \,, \tag{3}$$

$$\frac{\partial k}{\partial t} = \sigma_k \frac{\partial}{\partial y}\left(\nu \frac{\partial k}{\partial y}\right) + \nu \left(\frac{\partial u}{\partial y}\right)^2 - \beta_k \omega k \,, \tag{4}$$

$$\frac{\partial \omega}{\partial t} = \sigma_\omega \frac{\partial}{\partial y}\left(\nu \frac{\partial \omega}{\partial y}\right) + \Gamma \left(\frac{\partial u}{\partial y}\right)^2 - \beta_\omega \omega^2 \,, \tag{5}$$

where the constants $\sigma_k = \sigma_\omega = \frac{1}{2}$, $\beta_k = \frac{9}{100}$, $\beta_\omega = \frac{3}{40}$, $\Gamma = \frac{5}{9}$. The term g_x represents the downstream component of the gravitational acceleration on a slightly sloping ground. Equations (3), (4) and (5) describe the time evolution of the components of $\boldsymbol{T}$ due to the following factors.

2000 *Mathematics Subject Classification.* Primary: 58F39, 76F20; Secondary: 76B15.
Key words and phrases. k-ω turbulence, water waves, center manifold.
This work is supported by the Australian Research Council.

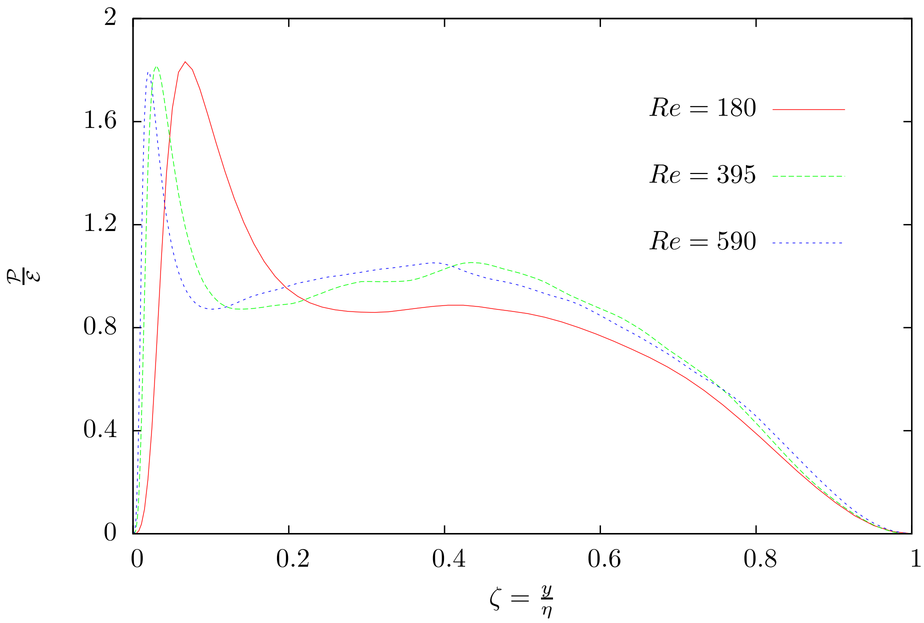

FIGURE 1. The ratio of production and dissipation of the energy for a fully developed 3D channel flow according to the DNS result of Moser et al. [5].

- Mixing due to turbulent eddies, represented by the operator $\mathcal{D} \equiv \frac{\partial}{\partial y}\left(\nu \frac{\partial}{\partial y}\right)$. This is the dominant factor governing the evolution of the vertical structure.
- Production of the kinetic energy and dissipation rate, represented by the terms $\mathcal{P}_k \equiv \nu(\partial u/\partial y)^2$ and $\mathcal{P}_\omega \equiv \Gamma(\partial u/\partial y)^2$. Their ratio is proportional to the turbulent mixing coefficient ν.
- Dissipation of the energy and dissipation rate, represented by the terms $\mathcal{E}_k \equiv beta_k \omega k$ and $\mathcal{E}_\omega \equiv beta_\omega \omega^2$. Their ratio is also proportional to ν.

From (4) and (5) follows

$$\frac{\mathcal{P}_k}{\mathcal{E}_k} \propto \frac{\mathcal{P}_\omega}{\mathcal{E}_\omega}\,. \tag{6}$$

2. **Boundary conditions.** Our model applies to fully developed turbulence which occupies the main body of the flow except a viscous sub-layer near the ground. Adjacent to the viscous sub-layer is an inertial sub-layer where the viscous effects are small in comparison with those of turbulence. There are many experimental results on turbulent quantities for fully developed channel flows [6, e.g.] which are the source for empirical relations for cross-flow profiles of $\boldsymbol{T}$. Using these results the values of $\boldsymbol{T}$ on the ground can be extrapolated and related to the 'friction velocity' $u_* = \sqrt{\nu\,\partial u/\partial y}$ and the height δ of the inertial sub-layer [4]. In our present modeling we aim to avoid the use of these empirical parameters and instead apply relevant physical criteria in order to clarify the implied capabilities of k-ω model (3), (4) and (5).

There is an approximate equality between the production $\mathcal{P}_k$ and dissipation $\mathcal{E}_k$ in the inertial sub-layer. There the ratio of production and dissipation of energy can be calculated using log-law [7]; this was verified by the DNS modeling of 3D fully developed turbulence by Moser et al. [5] (Figure 1). In the body of the flow up to distance δ from the ground the divergences of all statistical quantities are still negligible and the local rate of generation of turbulent energy $\mathcal{P}_k$ is equal to the rate of dissipation $\mathcal{E}_k$:

$$\mathcal{P}_k = \mathcal{E}_k \,. \tag{7}$$

With the increase of flow intensity, δ decreases (Figure 1). Therefore, instead of using an empirical value of δ, we assume (7) as the boundary condition on the ground:

$$\omega = \frac{1}{\sqrt{\beta_k}}\frac{\partial u}{\partial y}\,, \quad k = \frac{\nu}{\sqrt{\beta_k}}\frac{\partial u}{\partial y} \quad \text{on} \quad y = 0\,. \tag{8}$$

The value of u in the inertial sub-layer is proportional to u_*, and in the case of an hydraulically rough ground it is decreased due to the effects of local vorticity. To our knowledge there is no experimental data about the average effect of ground roughness on environmental flows. The scale of roughness may be many times the spatial scale of viscous effects. For simplicity, in the present modeling we assume that the value of u on the ground is small and is comparable to the error of modelling:

$$u \approx 0 \quad \text{on} \quad y = 0\,. \tag{9}$$

On the free surface we assume that wind stress is negligible, so the fluid surface is free of tangential stress,

$$\frac{\partial \boldsymbol{T}}{\partial y} = 0 \quad \text{on} \quad y = \eta\,. \tag{10}$$

3. **Centre manifold approach as a basis of the model.** The centre manifold approach is based on the difference in time scales of the turbulence: mixing, production and dissipation. Turbulent mixing is the dominant feature of the flow responsible for the vertical transport of $\boldsymbol{T}$. The production and dissipation of the energy are much slower and also local in space, therefore they are treated as perturbations to the turbulent mixing. Due to the difference in time scales, mixing is separated and treated alone, thus forming the leading terms of a series which approximates the solution of (3)–(5). The production and dissipation then cause relatively small time and space variations of the solution.

In order to apply centre manifold techniques we need to find equilibrium points of the dynamics of the purely turbulent mixing system

$$\frac{\partial \boldsymbol{T}}{\partial t} = \mathcal{D}(\boldsymbol{T})\,. \tag{11}$$

To find these equilibrium points for the dominant and long lasting case of mixing we need to solve

$$\mathcal{D}(\boldsymbol{T}) = 0\,. \tag{12}$$

There are six families of solutions of (12):

$$\boldsymbol{T} = \bar{\boldsymbol{T}} y^{(0,0,0)}\,, \quad \boldsymbol{T} \propto \bar{\boldsymbol{T}} y^{(1,0,0)}\,, \quad \boldsymbol{T} \propto \bar{\boldsymbol{T}} y^{(1,1,1)}\,, \tag{13}$$

$$\boldsymbol{T} \propto \bar{\boldsymbol{T}} y^{(0,1,1)}\,, \quad \boldsymbol{T} \propto \bar{\boldsymbol{T}} y^{\left(\frac{1}{2},\frac{1}{2},0\right)}\,, \quad \boldsymbol{T} \propto \bar{\boldsymbol{T}} y^{\left(0,\frac{1}{2},0,\right)}\,. \tag{14}$$

Each of these families provides three neutral modes of (12). The amplitudes of these modes are measured by the averages $\bar{\boldsymbol{T}} \equiv \left(\bar{u}, \bar{k}, \bar{\omega}\right)$:

$$\bar{\boldsymbol{T}} = \frac{1}{\eta}\int_0^\eta \boldsymbol{T}\,dy\,. \tag{15}$$

Consequently, the variables $\bar{\boldsymbol{T}}$ can be parameters of a slow manifold $\mathcal{M}_0$, provided that one of the families (13)–(14) is chosen by selecting appropriate boundary conditions. Then the evolution of $\boldsymbol{T}$ is expressed through the evolution of $\bar{\boldsymbol{T}}$, instead of directly in t, via the chain rule

$$\frac{\partial \boldsymbol{T}}{\partial t} = \frac{\partial \boldsymbol{T}}{\partial \bar{\boldsymbol{T}}}\dot{\bar{\boldsymbol{T}}}\,. \tag{16}$$

The derivative $\partial \boldsymbol{T}/\partial \bar{\boldsymbol{T}}$ is largely determined by the choice of families (13)–(14): we choose the first one of (13) which is y-independent and is therefore simplest. Then the relation between the $\boldsymbol{T}$ field and the amplitudes $\bar{\boldsymbol{T}}$ is simply

$$\boldsymbol{T} = \bar{\boldsymbol{T}} \Rightarrow \frac{\partial \boldsymbol{T}}{\partial \bar{\boldsymbol{T}}} = 1 \Rightarrow \frac{\partial \boldsymbol{T}}{\partial t} = \dot{\bar{\boldsymbol{T}}}\,. \tag{17}$$

The boundary conditions that generate these neutral modes are

$$\frac{\partial \boldsymbol{T}}{\partial y} = 0 \quad \text{on} \quad y = 0 \quad \text{and} \quad y = \eta\,. \tag{18}$$

We base the analysis on these boundary conditions, but with systematic modifications to meet the earlier physical boundary conditions.

Centre manifold theory [2, 8, 1, e.g.] assures that under modifying perturbations there exists a 3D slow manifold $\mathcal{M}_0$ parameterized by $\bar{\boldsymbol{T}}$.

4. **Implementation of physical boundary conditions.** The slow manifold $\mathcal{M}_0$ exists at the artificial equilibria of uniform turbulent properties defined by (11). These equilibria are based on the set boundary conditions (18). However, in our k-ω model we need the physical boundary conditions (8) and (9).

Thus we implement a smooth transition from the problem with the artificial boundary conditions to the physical problem where the ground significantly affects the turbulence. This transition 'bends' $\mathcal{M}_0$ and the resultant slow manifold $\mathcal{M}_1$ is also attractive.

To encompass both types of boundary condition we introduce a modelling parameter γ which ranges between $\gamma = 0$, corresponding to the slow manifold $\mathcal{M}_0$, and $\gamma = 1$, corresponding to the physical boundary conditions and supporting the centre manifold $\mathcal{M}_1$:

$$(1-\gamma)\frac{\partial u}{\partial y} = \gamma\frac{u}{\eta} \quad \text{on} \quad y = 0\,, \tag{19}$$

$$(1-\gamma)\frac{\partial k}{\partial y} = \gamma\left(k - \frac{\nu\frac{\partial u}{\partial y}}{\sqrt{\beta_k}}\right)\frac{1}{\eta} \quad \text{on} \quad y = 0\,, \tag{20}$$

$$(1-\gamma)\frac{\partial \omega}{\partial y} = \gamma\left(\omega - \frac{\frac{\partial u}{\partial y}}{\sqrt{\beta_k}}\right)\frac{1}{\eta} \quad \text{on} \quad y = 0\,. \tag{21}$$

5. **Applying centre manifold to a model problem of pure diffusion.** Our hypothesis is that there exists a smooth departure from the artificial slow manifold $\mathcal{M}_0$ to the 'bent' one $\mathcal{M}_1$ with physical boundary conditions on the ground, which will similarly attract exponentially quickly all solutions in its vicinity. To verify this hypothesis we compare the series' solution based on $\mathcal{M}_1$ with the analytical solution of the case of pure mixing (11) with the physical boundary conditions (8), (9) and (10).

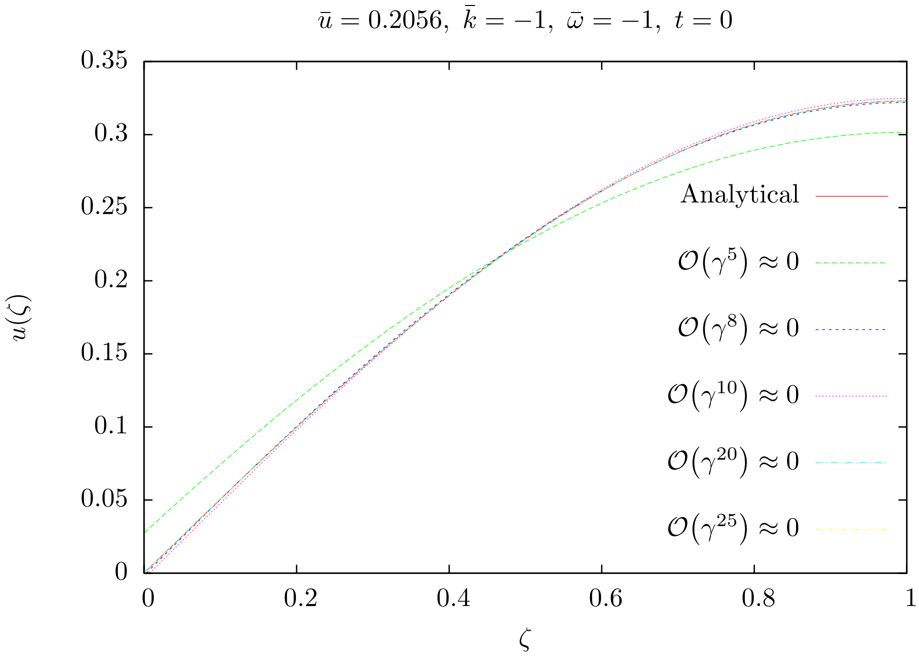

FIGURE 2. Comparison of analytical (37) and series' solutions for u.

5.1. **Analytical solution.** We solve (11) analytically for the case of

$$\nu \equiv \frac{k(t,y)}{\omega(t,y)} = \text{constant in } y\,. \tag{22}$$

Thus equations (11) become linear,

$$\begin{aligned} \frac{\partial u}{\partial t} &= \nu \frac{\partial^2 u}{\partial y^2}\,, \\ \frac{\partial k}{\partial t} &= \sigma_k \nu \frac{\partial^2 k}{\partial y^2}\,, \\ \frac{\partial \omega}{\partial t} &= \sigma_\omega \nu \frac{\partial^2 \omega}{\partial y^2}\,, \end{aligned} \tag{23}$$

and can be solved by separation of variables. By definition $\nu \equiv k/\omega$, therefore (22) imposes proportionality between spatial profiles of k and ω. Due to the separation of the variables we express the coefficient of proportionality in terms of $\bar{k}$ and $\bar{\omega}$, which are constants with respect to y:

$$\begin{aligned} u(t,y) &= \bar{u}(t)\mathcal{U}(y)\,, \\ \begin{bmatrix} k(t,y) \\ \omega(t,y) \end{bmatrix} &= \begin{bmatrix} \bar{k}(t) \\ \bar{\omega}(t) \end{bmatrix} \mathcal{K}(y)\,, \end{aligned} \tag{24}$$

where $\mathcal{K}(y)$ and $\mathcal{U}(y)$ are to be determined. The system (23) gives the time evolution of $\bar{\boldsymbol{T}}$:

$$\begin{aligned} \dot{\bar{u}}(t) &= \bar{u}(t)\nu(t)\frac{\mathcal{U}''(y)}{\mathcal{U}}\,, & (25)\\ \begin{bmatrix}\dot{\bar{k}}(t)\\ \dot{\bar{\omega}}(t)\end{bmatrix} &= \begin{bmatrix}\sigma_k\bar{k}(t)\\ \sigma_\omega\bar{\omega}(t)\end{bmatrix}\nu(t)\frac{K''(y)}{\mathcal{K}}\,. & (26)\end{aligned}$$

To obtain further knowledge on the time evolution of $\bar{\boldsymbol{T}}(t)$ we have to define the dependence of ν from time by differentiating (22):

$$\dot{\nu} = \frac{\dot{\bar{k}}\bar{\omega} - \bar{k}\dot{\bar{\omega}}}{\bar{\omega}^2} = (\sigma_k - \sigma_\omega)\,\frac{\bar{k}^2}{\bar{\omega}^2}\frac{\mathcal{K}''(y)}{\mathcal{K}}\,. \tag{27}$$

According the empirical data for k-ω model, $\sigma_k = \sigma_\omega = \frac{1}{2}$, therefore

$$\nu \equiv \frac{k(t,y)}{\omega(t,y)} = \text{constant in } t \text{ and } y\,. \tag{28}$$

By standard procedures we find $\mathcal{U}(y)$ and $\mathcal{K}(y)$ to be harmonic functions

$$\begin{aligned} \mathcal{U}(y) &= A_{\mathcal{U}}\cos(E_{\mathcal{U}}y) + B_{\mathcal{U}}\sin(E_{\mathcal{U}}y)\,, & (29)\\ \mathcal{K}(y) &= A_{\mathcal{K}}\cos(E_{\mathcal{K}}y) + B_{\mathcal{K}}\sin(E_{\mathcal{K}}y)\,, & (30)\end{aligned}$$

and $\bar{\boldsymbol{T}}$ exponentially decay:

$$\begin{aligned} \bar{u} &= \bar{u}(0)\exp(-\nu E_{\mathcal{U}}^2 t), & (31)\\ \bar{k} &= \bar{k}(0)\exp(-\sigma_k\nu E_{\mathcal{K}}^2 t), & (32)\\ \bar{\omega} &= \bar{\omega}(0)\exp(-\sigma_\omega\nu E_{\mathcal{K}}^2 t)\,. & (33)\end{aligned}$$

Applying the boundary conditions (9) and (10) for u and the normalization (15) for $\bar{u}$ we obtain

$$u(t,y) = \bar{u}(0)\exp\left(-\nu\frac{\pi^2}{4}t\right)\frac{\pi}{2}\sin\left(\frac{\pi}{2}y\right) = \bar{u}\frac{\pi}{2}\sin\left(\frac{\pi}{2}y\right). \tag{34}$$

Similarly for ω, the boundary condition on the ground (8) is

$$\omega\big|_{y=0} \equiv \bar{\omega}A_{\mathcal{K}} = \sqrt{\frac{1}{\beta_k}\left.\frac{\partial u}{\partial y}\right|_{y=0}} = \sqrt{\frac{1}{\beta_k}\bar{u}\frac{\pi^2}{4}}\,. \tag{35}$$

It requires synchronization in time between the $\bar{\omega}$ and $\bar{u}$:

$$\bar{\omega}(0)\exp(-\sigma_\omega\nu E_{\mathcal{K}}^2 t) \propto \bar{u}(0)\exp\left(-\nu\frac{\pi^2}{4}t\right) \Rightarrow E_{\mathcal{K}} = \frac{\pi}{2\sqrt{\sigma_\omega}}\,. \tag{36}$$

After applying the boundary conditions on the free surface (10) and the normalization for $\bar{k}$ and $\bar{\omega}$ the eventual analytical solution is

$$\begin{aligned} u(t,y) &= \bar{u}\frac{\pi}{2}\sin\left(\frac{\pi}{2}y\right)\,,\quad \text{where} & (37)\\ \bar{u}(t) &= \bar{\omega}(0)\frac{4\sqrt{\beta_k}}{\pi^2}E_{\mathcal{K}}\cot(E_{\mathcal{K}})\exp\left(-\nu\frac{\pi^2}{4}t\right)\,, & (38)\\ \begin{bmatrix}k(t,y)\\ \omega(t,y)\end{bmatrix} &= \begin{bmatrix}\bar{k}(t)\\ \bar{\omega}(t)\end{bmatrix}E_{\mathcal{K}}[\cot(E_{\mathcal{K}})\cos(E_{\mathcal{K}}y) + \sin(E_{\mathcal{K}}y)]\,,\quad \text{where} & (39)\\ \begin{bmatrix}\bar{k}(t)\\ \bar{\omega}(t)\end{bmatrix} &= \begin{bmatrix}\bar{k}(0)\\ \bar{\omega}(0)\end{bmatrix}\exp(-\sigma\nu E_{\mathcal{K}}^2 t)\,. & (40)\end{aligned}$$

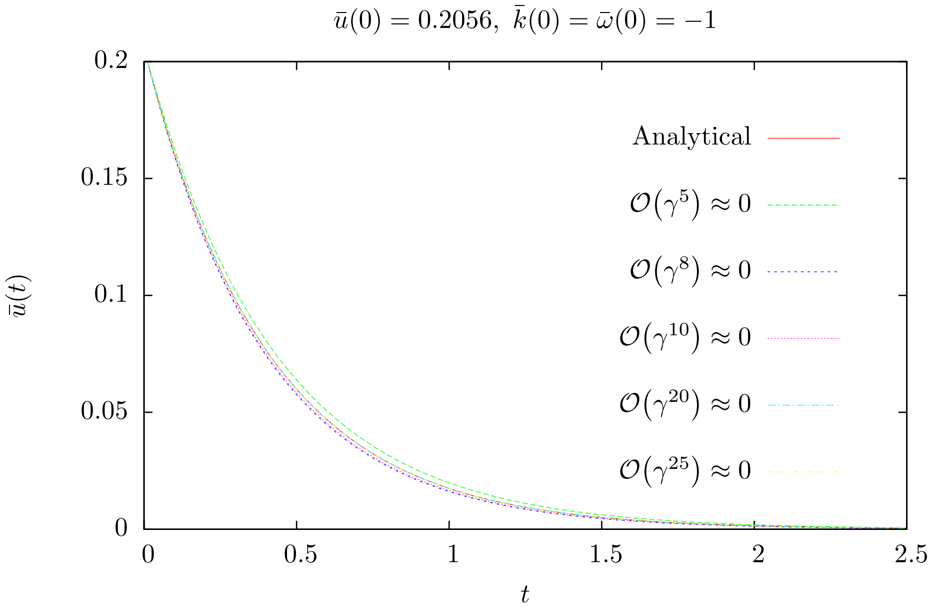

FIGURE 3. Comparison of analytical (31) and series' solutions for $\bar{u}$.

The system of equations (23) has two degrees of freedom since we have two independent input parameters $\bar{k}(0)$ and $\bar{\omega}(0)$. However, such a choice is not unique, the degrees of freedom can be measured by other two parameters of the model. We have chosen $\bar{k}(0)$ and $\bar{\omega}(0)$ since their ratio expresses the coefficient of diffusion $\nu = \bar{k}(0)/\bar{\omega}(0)$, which helps the analysis.

5.2. **Solution by centre manifold technique.** The approximate slow manifold $\mathcal{M}_1$ is constructed algebraically using computer algebra. The solutions for the turbulent fields $\boldsymbol{T}$ and the time evolution of the mean quantities $\bar{\boldsymbol{T}}$ involve polynomials in $\zeta = y/\eta$, the normalized vertical coordinate, and $\bar{\boldsymbol{T}}$. The coefficients of these polynomials are in turn polynomials in the ground condition parameter γ. The accuracy of these coefficients depends on the truncation in γ.

The computed series for the vertical structure $\boldsymbol{T}$ of the turbulence for the physical case $\gamma = 1$, to errors $\mathcal{O}(\gamma^5)$, are

$$u = \bar{u} f_1(\zeta), \tag{41}$$

$$\begin{bmatrix} k \\ \omega \end{bmatrix} = \begin{bmatrix} \bar{k} \\ \bar{\omega} \end{bmatrix} \left\{ f_1(\zeta) + \frac{\bar{u}}{\bar{\omega}} \frac{1}{\beta_k} f_2(\zeta) \right\}, \tag{42}$$

where

$$f_1(\zeta) = 0.1334 + 2.3386\,\zeta - 0.531\,\zeta^2 - 0.6037\,\zeta^3 + 0.1083\,\zeta^4 + 0.025\,\zeta^5 - 0.0037\,\zeta^6 - 0.0001984\,\zeta^7 + 2.48 \cdot 10^{-5}\,\zeta^8 \approx \frac{\pi}{2} \sin\left(\frac{\pi}{2}\zeta\right), \tag{43}$$

$$f_2(\zeta) = 1.4074 - 3.58\,\zeta + 0.211\,\zeta^2 + 1.5\,\zeta^3 - 0.278\,\zeta^4 - 0.0583\,\zeta^5 + 0.009722\,\zeta^6\,. \tag{44}$$

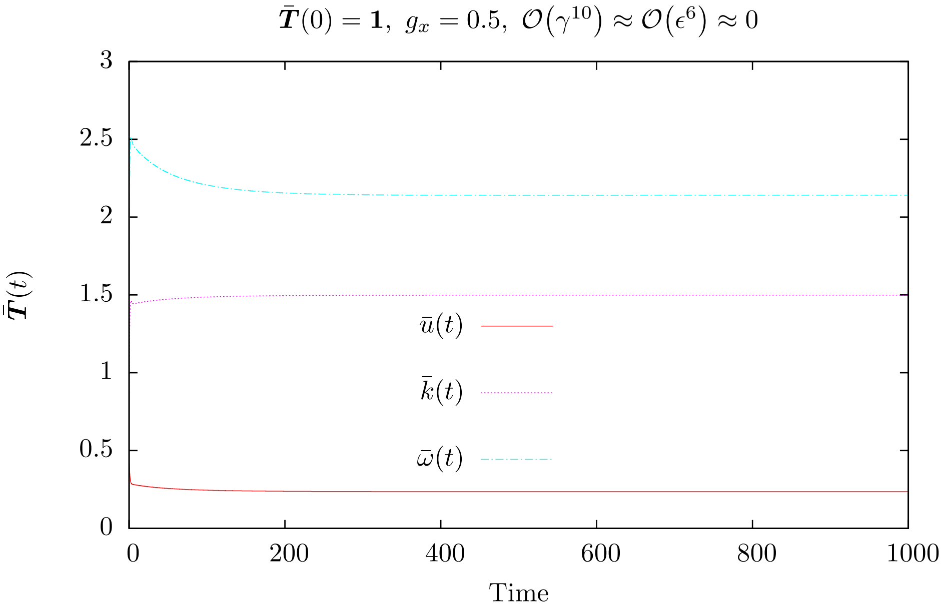

FIGURE 4. Convergence of $\bar{\boldsymbol{T}}(t)$ to the stationary state.

Correspondingly, the dynamics of the amplitudes $\bar{\boldsymbol{T}}$ are governed by the approximation, computed to terms $\mathcal{O}(\gamma^{25})$ and evaluated at the physically relevant $\gamma = 1$,

$$\begin{aligned} \dot{\bar{u}} &= -2.4674\,\frac{\bar{k}}{\bar{\omega}\eta^2}\bar{u}, \\ \begin{bmatrix} \dot{\bar{k}} \\ \dot{\bar{\omega}} \end{bmatrix} &= \begin{bmatrix} \bar{k} \\ \bar{\omega} \end{bmatrix} \left(-1.2337\frac{\bar{k}}{\bar{\omega}} + 6.1544\frac{\bar{k}}{\bar{\omega}}\frac{\bar{u}}{\bar{\omega}} \right), \end{aligned} \tag{45}$$

and according to (35) the ratio $\bar{u}/\bar{\omega}$ is constant in time.

Solving these ordinary differential equations gives

$$\begin{aligned} \bar{u} &= \bar{u}(0)\exp\left(-2.4674\frac{\bar{k}}{\bar{\omega}\eta^2}t \right), \\ \begin{bmatrix} \bar{k} \\ \bar{\omega} \end{bmatrix} &= \begin{bmatrix} \bar{k}(0) \\ \bar{\omega}(0) \end{bmatrix} \exp\left[\left(-1.2337 + 6.1544\,\frac{\bar{u}(0)}{\bar{\omega}(0)} \right) \frac{\bar{k}}{\bar{\omega}\eta^2}t \right]. \end{aligned} \tag{46}$$

A comparison of the above slow manifold solution with the analytical solution is shown in Figure 2 and Figure 3. The spatial profiles of u by the two methods are close. The decay curves of $\bar{u}$ are also close. Observe that the spatial profile by the series matches the analytical result satisfactorily when the truncation power of γ is larger than five.

6. **Applying centre manifold technique to k-ω model.** The analysis of the previous section applies only to the process of turbulent mixing. The terms of production, dissipation and gravitational acceleration 'bend' the manifold $\mathcal{M}_1$ to nearby manifold $\mathcal{M}_2$ of slow evolution. We treat these terms as perturbations of order ϵ with the case $\epsilon = 0$ corresponding to the 'pure mixing' manifold $\mathcal{M}_1$ and

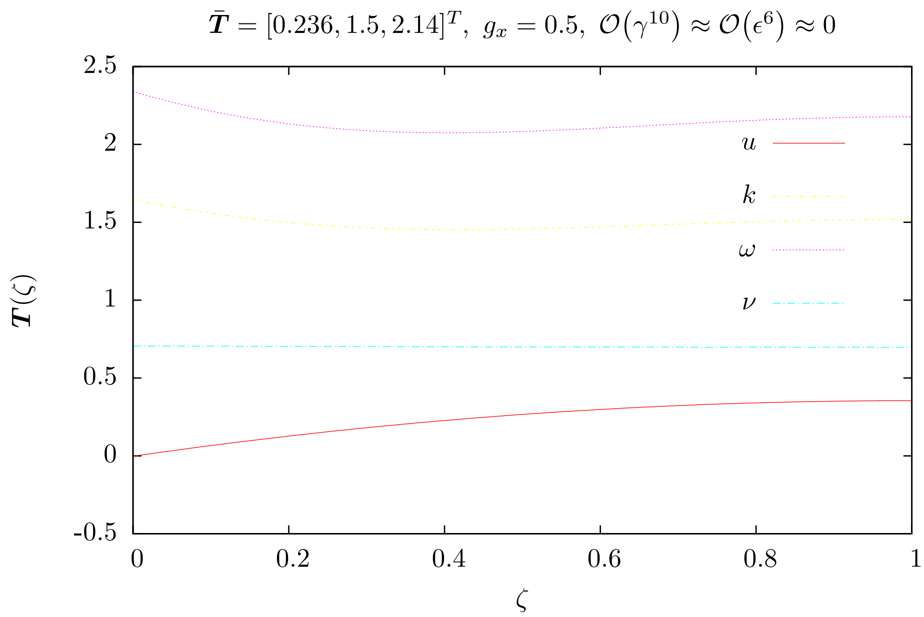

FIGURE 5. Cross-flow profiles of $\boldsymbol{T}$ in steady state.

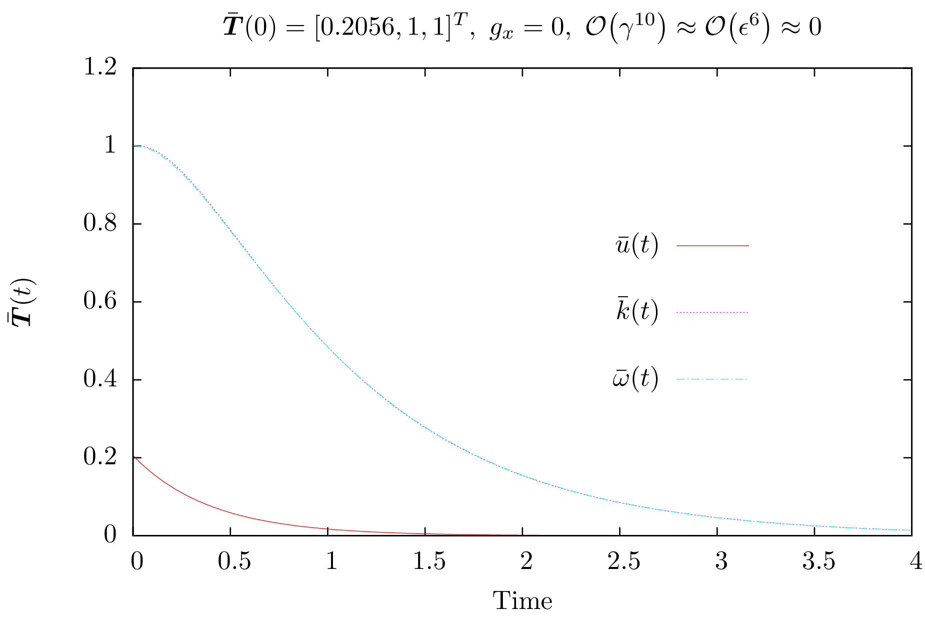

FIGURE 6. The decay of $\bar{\boldsymbol{T}}(t)$ for horizontal flow.

the case $\epsilon = 1$ corresponding to the k-ω manifold $\mathcal{M}_2$. The accuracy of $\mathcal{M}_2$ is controlled by the power of ϵ retained in the computer algebra construction.

The leading terms of the series governing the time evolution of $\bar{T}$ on $\mathcal{M}_2$ are

$$\dot{\bar{u}} = -2.4674\,\frac{\bar{k}}{\bar{\omega}\eta^2}\bar{u} + 0.82176\,g_x\,, \tag{47}$$

$$\dot{\bar{k}} = -1.2337\,\frac{\bar{k}^2}{\bar{\omega}\eta^2} + 2.1844\,\frac{\bar{k}}{\bar{\omega}\eta}\,g_x + 6.1544\,\frac{\bar{k}^2}{\bar{\omega}^2\eta^3}\bar{u} - 0.1263\,\bar{k}\bar{\omega} + 0.7365\,\frac{\bar{k}\bar{u}}{\eta}\,, \tag{48}$$

$$\dot{\bar{\omega}} = -1.2337\,\frac{\bar{k}}{\eta^2} + 2.1844\,\frac{g_x}{\eta} + 6.1544\,\frac{\bar{k}}{\bar{\omega}\eta^3}\bar{u} - 0.1055\,\bar{\omega}^2 + 0.636\,\frac{\bar{\omega}\bar{u}}{\eta}\,. \tag{49}$$

Compare (49) for manifold $\mathcal{M}_2$ with (46) for manifold $\mathcal{M}_1$: the bending of $\mathcal{M}_1$ under the gravitational term g_x, production term $\mathcal{P}$ and dissipation term $\mathcal{E}$ of the k-ω model, causes the generation of a multitude of additional terms into the model.

Under the adopted boundary conditions (10), (8) and (9) there exists a unique non-zero stationary solution for the amplitudes $\bar{\boldsymbol{T}}$. Figure 4 shows the convergence of the numerical solution of (49) to this steady state. It also demonstrates stability of this state.

This stationary solution corresponds to the physical flow on an inclined plane forced by gravity and counterbalanced by turbulent viscosity ν. The computed average velocity, energy and dissipation rate in the steady state are

$$\bar{u} = 0.334\sqrt{g_x\,\eta}\,,\quad \bar{k} = 3\,g_x\,\eta\,,\quad \bar{\omega} = 3.03\sqrt{\frac{g_x}{\eta}}\,. \tag{50}$$

The corresponding vertical distribution of the turbulent properties $\boldsymbol{T}$ is shown in Figure 5.

The case $g_x = 0$ corresponds to the decay of horizontal flow slowed down by the turbulent friction. This case is illustrated by Figure 6.

REFERENCES

[1] A. J. Roberts, *Low-dimensional modelling of dynamical systems applied to some dissipative fluid mechanics*, In Rowena Ball and Nail Akhmediev, editors, Nonlinear dynamics from lasers to butterflies, volume 1 of "Lecture notes in complex systems," World Scientific, (2003), 257–313.

[2] J. Carr, *Applications of centre manifold theory*, volume 35 of "Applied Mathematical Sciences," Springer-Verlag, 1981.

[3] Lars Davidson, *An introduction to turbulence models*, Technical Report 97/2, Chalmers University of Technology, Department of thermo and fluid dynamics, November, 2003.

[4] D. J. Georgiev, A. J. Roberts, and D. V. Strunin, *The dynamics of the vertical structure of turbulence in flood flows*, ANZIAM Journal, In press, 2007.

[5] R. D. Moser, J. Kim, and N. N. Mansour. *Direct numerical simulation of turbulent channel flow up to* $Re_\tau = 590$, Physics of fluids, **11**(4) (1999), 943–945.

[6] Iehisa Nezu. *Open-channel flow turbulence and its research prospects in the 21st century*, Journal of Hydraulic Engineering, **131**(4) April (2005), 229–246.

[7] David C. Wilcox. "Turbulence modeling for CFD," DCW Industries Inc, La Canada, California, second edition, 1998.

[8] Y.A.Kuznetsov. *Elements of applied bifurcation theory*, Applied Mathematical Sciences, Springer-Verlag, **112** (1995).

Received September 2006; revised May 2007.

E-mail address: strunin@usq.edu.au